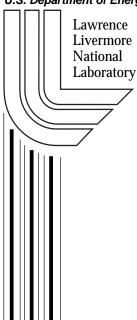
Measuring spherical harmonic coefficients on a sphere

S. M. Pollaine

Anomalous Absorption Conference Lake Placid, New York June 22-27, 2003

May 16, 2003

U.S. Department of Energy



DISCLAIMER

This document was prepared as an account of work sponsored by an agency of the United States Government. Neither the United States Government nor the University of California nor any of their employees, makes any warranty, express or implied, or assumes any legal liability or responsibility for the accuracy, completeness, or usefulness of any information, apparatus, product, or process disclosed, or represents that its use would not infringe privately owned rights. Reference herein to any specific commercial product, process, or service by trade name, trademark, manufacturer, or otherwise, does not necessarily constitute or imply its endorsement, recommendation, or favoring by the United States Government or the University of California. The views and opinions of authors expressed herein do not necessarily state or reflect those of the United States Government or the University of California, and shall not be used for advertising or product endorsement purposes.

This is a preprint of a paper intended for publication in a journal or proceedings. Since changes may be made before publication, this preprint is made available with the understanding that it will not be cited or reproduced without the permission of the author.

This report has been reproduced directly from the best available copy.

Available electronically at http://www.doc.gov/bridge

Available for a processing fee to U.S. Department of Energy
And its contractors in paper from
U.S. Department of Energy
Office of Scientific and Technical Information
P.O. Box 62
Oak Ridge, TN 37831-0062

Telephone: (865) 576-8401 Facsimile: (865) 576-5728 E-mail: reports@adonis.osti.gov

Available for the sale to the public from U.S. Department of Commerce National Technical Information Service 5285 Port Royal Road Springfield, VA 22161 Telephone: (800) 553-6847

Facsimile: (703) 605-6900 E-mail: orders@ntis.fedworld.gov

Online ordering: http://www.ntis.gov/ordering.htm

OR

Lawrence Livermore National Laboratory Technical Information Department's Digital Library http://www.llnl.gov/tid/Library.html

Measuring spherical harmonic coefficients on a sphere

S.M. Pollaine

Lawrence Livermore National Laboratory, Livermore, California 94551-9900

The eigenfunctions of Rayleigh-Taylor modes on a spherical capsule are the spherical harmonics $Y_{l,m}$ These can be measured by measuring the surface perturbations along great circles and fitting them to the first few modes by a procedure described in this article. For higher mode numbers, it is more convenient to average the Fourier power spectra along the great circles, and then transform them to spherical harmonic modes by an algorithm derived here.

I. Introduction

The Rayleigh-Taylor instability [1,2] can have a drastic impact on the implosion of an inertial confinement fusion (ICF) capsule. Small perturbations on the capsule surface may grow into large perturbations during the implosion. This growth will degrade capsule yield if significant mixing occurs, or if the imploding high-density shell breaks up. Thus it is important to accurately predict the growth of these perturbations to determine the required smoothness for ICF capsules.

Any computational model for predicting perturbation growth, such as the Haan model [3], must start with the spectrum of spherical harmonic modes that represents the initial surface perturbations. Each mode is grown by a factor that is determined from two-dimensional hydrodynamic simulations. Then the growth of each mode is limited by a non-linear saturation model. The final sum over modes gives the predicted final configuration of the capsule surface. Thus it's important to measure the spectrum of spherical harmonic modes, which is inherently two dimensional.

There are two main ways to measure the modal spectrum. The most direct way (although not usually done) is to measure the surface perturbations at many points around the sphere, and fit to a set of modes. This fit is mathematically described in part II. The most common way is to measure the surface perturbations along a great circle, obtain one-dimensional modes by a Fourier transformation, and convert these values to the two-dimensional spherical harmonic modal spectrum. Part III shows how to make that transformation with isotropic perturbations, and Part IV

discusses the anisotropic case of axisymmetric perturbations. We argue in Part V that the most efficient way to obtain a modal spectrum is a combination of these two ways, and show results with with numerical experiments. Part VI discusses the case of an isolated defect.

II. Direct fit to surface perturbations

Let $\{\Omega i\}$, i=1,...,N, be a set of solid angles at which height $\{Ri\}$ is measured. The set $\{\Omega i\}$ could be, for instance, a collection of great circle traces on the sphere. We want to find the spherical harmonic coefficients a_{lm} that are the best fit to $R_i = \sum_{lm} a_{l,m} Y_{l,m}(\Omega_i), l \le l_{max}$, where $-l \le m \le l$ and $0 \le l \le l_{max}$

To get the best fit, we will minimize

$$I = \frac{1}{2} \sum_{i=1}^{N} \left(\sum_{l,m}^{l_{\text{max}}} \left(a_{l,m} Y_{l,m}(\Omega_i) \right) - R_i \right)^2 \text{ by setting its partial derivatives with respect to } a_{\text{lm}} \text{ to zero:}$$

$$\sum_{i=1}^{N} \left(\sum_{p,q}^{l_{\text{max}}} \left(a_{p,q} Y_{p,q} \left(\Omega_{i} \right) \right) - R_{i} \right) Y_{l,m} \left(\Omega_{i} \right) = 0$$

or, rewriting,

$$\sum_{p,q}^{l_{\max}} a_{p,q} \left(\sum_{i=1}^{N} Y_{p,q} (\Omega_i) Y_{l,m} (\Omega_i) \right) = \sum_{i=1}^{N} R_i Y_{l,m} (\Omega_i)$$

Thus we get a set of $(l_{\text{max}} + 1)^2$ equations with $(l_{\text{max}} + 1)^2$ unknowns, namely the coefficients a_{lm} . These equations are easily solved by matrix inversion, as long as the number of points N is greater than $(l_{\text{max}} + 1)^2$ (otherwise, the matrix is singular).

For randomly distributed points, and in the presence of random Gaussian noise with an rms of σ_n , simulations show that the error in a typical a_{lm} coefficient is roughly $\frac{\sigma_n}{\sqrt{N-(l_{max}-1)^2}}$ when N- $(l_{max}-1)^2$ is greater than about 10 or so.

However, there is an issue of where the points are located. If large areas of the sphere have no sample points, then this algorithm will not work well. We get best results when the points $\{\Omega i\}$ are scattered around the sphere rather than being clumped together. N points scattered randomly around the sphere allows this algorithm to work up to mode $\sqrt{N} - 1$.

II a. Great circle measurements

It is usually most convenient to measure surface perturbations along great circles on the sphere. If we collect points from three mutually perpendicular great circles, then simulations show this algorithm is only accurate up to mode 2. In these simulations, we constructed a set of perturbations along the great circles by building up a set of spherical harmonics, with random phases and pre-determined amplitudes, so that the modal spectrum was defined in advance. This is described in greater detail in section Va below. We then used the technique describe above to derive a spectrum from the constructed perturbations along the great circles. An attempt to fit modes 1 and 2, which have 8 independent coefficients, gave the expected spectrum. An attempt to fit modes1 through 3, which have 15 independent coefficients, gave nonsensical results.

More circles allow the measurements of more modes. In what follows, we will describe the great circles by the location of their poles. For example, three mutually perpendicular circles have their poles located at the six faces of a cube.

The eight corners of a cube describe four great circles, which allow the measurements up to and including mode 3.

The 12 faces of a dodecahedron define 6 great circles, which allow the measurements up to and including mode 5.

The 20 faces of an icosahedron define 10 great circles, which allow the measurements up to mode 9.

The 60 faces of a soccer ball define 30 great circles, which allow the measurements up to and including mode 29.

Simulations with nine great circles, defined by the intersection of a sphere with the nine planes x=0, y=0, z=0, x=y, x=z, y=z, x=-y, y=-z and x=-z, show that this algorithm works up to and including mode 9.

These results are summarized in Table I below. For each case, we also determined the minimum number of points per great circle needed to measure the given number of modes. Note that the maximum mode that can be measured is one less than the number of great circles.

Table I

# Great circles	Max mode	Minimum pts/circle
3	2	4
4	3	7
6	5	11

9	8	11
10	9	15
30	29	35

We added random Gaussian noise to the simulations, in the form of an uncorrelated error added to every point, with rms σ . The errors in each spectral element was σ/\sqrt{N} , where N was the total number of points = number of great circles times the number of points in each circle. The results were the same, whether the errors came from random Gaussian noise, or from modes larger than the maximum mode being fit.

III. Converting 1-D spectra into 2-D spectra

For high mode numbers, the number of points on the sphere needed to specify the spectrum grows quadratically with maximum mode number. For mode numbers greater than about 10, it is more convenient to measure the surface perturbations along a great circle, take the Fourier transform to get the 1-D power spectrum, and convert the 1-D spectrum into the 2-D power spectrum defined by the spherical harmonics. The algorithm to make this conversion [4] is derived below, assuming that the surface perturbations are isotropic. We will also show the conversion for the anisotropic case when the perturbations are axially symmetric.

In this derivation, we derive expressions for both P_{1d} and P_{2d} , the 1-D and 2-D power spectra. Then we derive the relationship between them, so that the P_{2d} needed for computer models can be derived from the measured P_{1d} .

III a: Two-Dimensional Power Spectrum

The initial surface spectrum is described by a surface-height function $f(\Omega)$, which is expressed as a sum of spherical harmonics:

$$f(\Omega) = \sum_{l,m} Y_{l,m}(\Omega) \quad , \tag{1}$$

where l runs from 0 to ∞ and m runs from -l to l. The coefficients $R_{l,m}$ are given by

$$R_{l,m} = \int f(\Omega) Y_{l,m}^*(\Omega) d\Omega \tag{2}$$

For convenience, f will be defined relative to the average surface height, so that $\langle f(\Omega) \rangle = 0$ and thus $R_{0,0} = 0$. By picking the center of the sphere, we can also set $R_{1,m} = 0$, and start with l=2. For greater generality, we will start our sums with mode l=1, and the first term may or may not be zero. The total variance, in units of cm², is given by combining (1) and (2) to get

$$\langle f^{2}(\Omega) \rangle = \frac{1}{4\pi} \int f^{2}(\Omega) d\Omega$$

$$= \frac{1}{4\pi} \sum_{l,m} |R_{l,m}|^{2}$$
(3)

In what follows, we will assume that the perturbations are isotropic. This means that $\langle |R_{l,m}| \rangle$ is independent of m, where <> is used to denote an ensemble average over many similarly constructed capsules. We define the two-dimensional power spectrum $P_{2D}(l)$ as the contribution of each mode l to the total variance. Since there are 2l+1 values of m for each l, $P_{2D}(l)$ is given by

$$P_{2D}(l) = \frac{2l+1}{4\pi} \left\langle \left| R_{l,0} \right|^2 \right\rangle , \tag{4}$$

and the total variance is given by $\sum_{l=1}^{\infty} P_{2D}(l)$. The l=1 contribution again can be eliminated by choosing the center of the sphere. It is this power spectrum that is required in a computer simulation of instability growth.

III b: One-Dimensional Power Spectrum

In practice, the surface height on a capsule is usually measured along a onedimensional path, typically a great circle, and the power spectrum is taken to be the square of the absolute value of the Fourier transform of the height variation along the path. Let the height along a co-latitude θ_0 be given by

$$g(\phi) = f(\theta_0, \phi) = \sum_{n=-\infty}^{\infty} a_n e^{in\phi} \qquad , \tag{5}$$

where we will usually pick the great circle $\theta_0 = \pi/2$ and

$$a_n = a_{-n}^* = \frac{1}{2\pi} \int_{0}^{2\pi} g(\phi) e^{-in\phi} d\phi$$
 (6)

As in the two-dimensional case, we have taken $g(\phi)$ to be measured relative to the average surface height so that $a_0 = 0$, and we could choose to define the center of the sphere so that $a_1 = a_{-1} = 0$ as well. The variance of g is given by

$$\langle g^{2}(\phi) \rangle = \frac{1}{2\pi} \sum_{n=-\infty}^{\infty} \sum_{n=-\infty}^{\infty} a_{n} a_{n}^{*} \int_{0}^{2\pi} e^{in\phi} e^{-in'\phi} d\phi$$

$$= \sum_{n=-\infty}^{\infty} |a_{n}|^{2} = 2 \sum_{n=1}^{\infty} |a_{n}|^{2}$$
(7)

As in the two-dimensional case, we define P_{1D} as the contribution of each mode number n to the variance. From (7), this definition means

$$P_{1D}(n) = 2|a_n|^2$$
, (8)

with the total variance given by $\sum_{n=1}^{\infty} P_{1D}(n)$.

III c: Comparison of P_{2D} with P_{1D}

It is important to note that P_{1D} and P_{2d} are different, even though both represent the contribution to the total variance of surface perturbations per mode number 1. This difference comes about because the two-dimensional modes do not correspond to the one-dimensional modes. We now derive the relationship between P_{1D} and P_{2d} , assuming that the surface perturbations are isotropic. This will allow us to connect the experimentally measured spectra with those needed for numerical simulations.

In order to relate the two spectra, we first need to re-express the onedimensional coefficients a_n in terms of the coefficients $R_{l,m}$ of the twodimensional representation of the surface variation. For a given angle θ_0 , we can substitute the expansion of $f(\Omega)$ [Eq. (1)] into our definition of $g(\theta)$ [Eq. (5)] and a_n [Eq. (6)] to yield

$$a_n = \frac{1}{2\pi} \sum_{l,m} R_{l,m} \int_{0}^{2\pi} Y_{l,m}(\theta_0, \phi) e^{-in\phi} d\phi . \tag{9}$$

Further, the spherical harmonics are related to the associated Legendre polynomials $P_{l,m}$ by

$$Y_{l,m}(\theta,\phi) = \sqrt{\frac{2l+1}{4\pi} \frac{(l-m)!}{(l+m)!}} P_{l,m}(\cos\theta) e^{im\phi} . \tag{10}$$

Combining Eqs. (9) and (10) and integrating over ϕ gives

$$a_n = \sum_{l=n}^{\infty} R_{l,n} P_{l,n}(\cos \theta) \sqrt{\frac{2l+1}{4\pi} \frac{(l-m)!}{(l+m)!}} . \tag{11}$$

Now we combine Eqs. (4), (8) and (11), and the assumption of isotropy, which allows us to make the 11' terms disappear when we take the ensemble average:

$$\left\langle R_{l,n}R_{l',n}^{*}\right\rangle = \left|R_{l,n}\right|^{2}\delta_{l,l'}.$$

This yields

$$P_{1D}(n) = 2\sum_{l=n}^{\infty} P_{2D}(l) P_{l,n}^{2}(\cos\theta_{0}) \frac{(l-n)!}{(l+n)!} .$$
 (12)

For the usual case of a great circle trace, $\theta_0 = \pi/2$ and

$$P_{l,m}(0) = \begin{cases} (-1)^{(l+m)/2} \frac{(l+m-1)!!}{(l-m)!!} (l+m \text{ even}) \\ 0 \qquad (l+m \text{ odd}) \end{cases}$$
 (13)

Substituting Eq. (13) into (12) gives the desired relationship between P_{1D} and P_{2d} :

$$P_{1D}(n) = \sum_{l=n,n+2,...}^{\infty} U_{nl} P_{2D}(l), \quad U_{nl} = 2 \frac{(l-n-1)!! (l+n-1)!!}{(l-n)!! (l+n)!!}$$
(14)

This can be inverted to obtain

$$P_{2D}(l) = \sum_{n=l+1}^{\infty} V_{ln} P_{lD}(n), \quad V_{ln} = -(2l+1)n \frac{(n+l-2)!! (n-l-3)!!}{(n+l+1)!! (n-l)!!}$$
(15)

or, in another form,

$$P_{2D}(l) = (l + \frac{1}{2}) \sum_{n=l,l+2,\dots}^{\infty} \left[P_{1D}(n) - P_{1D}(n+2) \right] \frac{(n+l)!! (n-l-1)!!}{(n+l+1)!! (n-l)!!} . \tag{16}$$

In evaluating the double factorials for negative values, we use (-3)!! = -1 and (-2)!! = (-1)!! = 0!! = 1. The first few terms of Eq. (14) are

$$\begin{split} P_{1D}(1) &= P_{2D}(1) + \frac{3}{8}P_{2D}(3) + \frac{15}{64}P_{2D}(5) + \dots \\ P_{1D}(2) &= \frac{3}{4}P_{2D}(2) + \frac{5}{16}P_{2D}(4) + \frac{105}{512}P_{2D}(6) + \dots \\ P_{1D}(3) &= \frac{5}{8}P_{2D}(3) + \frac{35}{128}P_{2D}(5) + \frac{189}{1024}P_{2D}(7) + \dots \\ P_{1D}(4) &= \frac{35}{64}P_{2D}(4) + \frac{63}{256}P_{2D}(6) + \frac{693}{4096}P_{2D}(8) + \dots \end{split}$$

and of Eq. (15) are

$$\begin{split} P_{2D}(1) &= P_{1D}(1) - \frac{3}{5} P_{1D}(3) - \frac{1}{7} P_{1D}(5) - \dots \\ P_{2D}(2) &= \frac{4}{3} P_{1D}(2) - \frac{16}{21} P_{1D}(4) - \frac{4}{21} P_{1D}(6) - \dots \\ P_{2D}(3) &= \frac{8}{5} P_{1D}(3) - \frac{8}{9} P_{1D}(5) - \frac{112}{495} P_{1D}(7) - \dots \\ P_{2D}(4) &= \frac{64}{35} P_{1D}(4) - \frac{384}{385} P_{1D}(6) - \frac{256}{1001} P_{1D}(8) - \dots \end{split}$$

These expressions are exact, but cumbersome, and are useful for numerical calculations. Alternative integral representations are useful for mode numbers above 10 or so. By using Stirling's approximation for factorials and double factorials, good for large values of x,

$$x! = \sqrt{2\pi x} (x/e)^x , \qquad (17)$$

$$x!! = \begin{cases} \sqrt{\pi x} (x/e)^{x/2} & (x \ even) \\ \sqrt{2x} (x/e)^{x/2} & (x \ odd) \end{cases},$$
 (18)

equations (14) and (16) become the integral equations

$$P_{1D}(n) = \frac{2}{\pi} \int_{n}^{\infty} \frac{P_{2D}(l) \, dl}{\sqrt{l^2 - n^2}}$$
 (19)

$$P_{2D}(l) = -l \int_{l}^{\infty} \frac{dn}{\sqrt{n^2 - l^2}} \frac{d}{dn} P_{1D}(n)$$
 (20)

(Eq. (15) leads to the integral
$$P_{2D}(l) = -\frac{2l+1}{2} \int_{l}^{\infty} \frac{P_{1D}(n) n \, dn}{\left(n^2 - l^2\right)^{3/2}}$$
), which is

divergent when $n \sim 1$, where the continuum approximation breaks down.)

Another form for Eq. (20) is obtained by multiplying (19) by $n/\sqrt{n^2-k^2}$ and integrating from k to ∞ . Interchanging the order of integration on the right hand side, using

$$\int_{k}^{l} \frac{n \, dn}{\sqrt{l^2 - n^2} \sqrt{n^2 - k^2}} = \frac{\pi}{2} \tag{21}$$

and differentiating both sides gives an additional integral form:

$$P_{2D}(l) = -\frac{d}{dl} \int_{-l}^{\infty} dn \frac{n P_{1D}(n)}{\sqrt{n^2 - l^2}}$$
 (22)

With a change of variables, we obtain a third, and perhaps the most useful, form as well:

$$P_{2D}(l) = -\frac{d}{dl} \int_{0}^{\infty} P_{1D}(\sqrt{l^2 + n^2}) dn$$
 (23)

All of these integral representations are good for large n and l, and break down for n and l below 5 or 10, where the discreteness of the modes becomes very important.

IV. Anisotropic perturbations

It is interesting to compare these results to the maximally anisotropic case of a sphere with azimuthally symmetric perturbations. This would approximate the case of a sphere turned on a lathe, where the variations would be mostly in the θ direction and not in the ϕ direction. In this case,

the perturbations are described by $f(\theta)$ along any line of longitude, with θ varying from 0 to π . We then have the choice of expanding $f(\theta)$ in a Fourier series with $\cos(n\theta)$ terms only, or in spherical harmonics, with m=0 terms only. In that case, it becomes more convenient to use Legendre polynomials, which are related to the spherical harmonics by Eq. (10) with m=0. Thus we have

$$f(\theta) = \sum_{n=1}^{\infty} a_n \cos(n\theta) = \sum_{l=1}^{\infty} b_l P_l(\cos(\theta)) , \qquad (24)$$

with
$$P_{1D}(n) = 2a_n^2$$
 and $P_{2D}(l) = \frac{b_l^2}{2l+1}$ (25)

With the orthogonality relations

$$\int_{0}^{\pi} \cos(m\theta) \cos(n\theta) d\theta = \frac{\pi}{2} \delta_{mn}$$

$$\int_{-1}^{1} P_{l}(\cos(\theta)) P_{m}(\cos(\theta)) d\cos(\theta) = \frac{2}{2l+1} \delta_{lm}$$

we have

$$a_{n} = \frac{2}{\pi} \int_{0}^{\pi} f(\theta) \cos(n\theta) d\theta$$

$$b_{l} = \frac{2l+1}{2} \int_{-1}^{1} f(\theta) P_{l}(\cos(\theta)) d\cos(\theta)$$
(26)

The desired power spectrum can be obtained from (25) and (26) in two ways. (1) Obtain b_1 directly, calculating the Legendre polynomials by using the recursion relation $P_0(x) = 1$, $P_1(x) = x$, and $nP_n(x) - (2n-1)xP_{n-1}(x) + (n-1)P_{n-2}(x) = 0$. (2) Obtain the set a_n from a Fourier transform, then convert to b_1 by using

$$\cos(n\theta) = \sum_{l=0}^{n} U_{nl} P_{l}(\cos(\theta)), \quad n-l \text{ even}, \quad U_{nl} = \frac{2l+1}{2} \int_{-1}^{1} \cos(n\theta) P_{l}(\cos(\theta)) d\cos\theta$$

$$P_{l}(\cos(\theta)) = \sum_{l=0}^{l} V_{ln} \cos(n\theta), \quad n-l \text{ even}, \quad V_{ln} = \frac{2}{\pi} \int_{0}^{\pi} \cos(n\theta) P_{l}(\cos(\theta)) d\theta$$
(27)

The coefficients U_{nl} and V_{ln} are given by the expressions in Eqs. (14) and (15)! It follows that

$$a_{n} = \sum_{i=0}^{n} U_{nl} b_{l}, \quad n-l \text{ even}$$

$$b_{l} = \sum_{i=0}^{l} V_{ln} a_{n}, \quad l-n \text{ even}$$

$$(28),$$

where again U_{nl} and V_{ln} are given by the expressions in Eqs. (14) and (15).

V. Combining two ways of measuring perturbations

The two ways of measure surface perturbations is the direct way, described in part II, and the usual way that converts the Fourier transforms of great circles to the two-dimensional power spectrum, described in part III.

Typically, measurements are made along various great circles. A great circle trace will measure thousands of points, but these are not uniformly distributed over the sphere. One great circle can not even measure mode 1 relative to a fixed center. Three mutually perpendicular great circles can measure modes 1 and 2, but not mode 3. N great circles allow the measurements of up to mode N-1, provided that these circles are "reasonably distributed" around the sphere. Thus, the direct way described in part II can only be done up to mode 2 for the usual three mutually perpendicular great circles, and up to mode 8 for the nine great circles inscribed in the planes x=0, y=0, z=0, x=y, x=-y, x=-z, y=z and y=-z.

In Part III, we used the assumption of isotropy in two ways: $\langle R_{l,n}R_{l',n}^*\rangle = |R_{l,n}|^2 \delta_{l,l'}$ and $\langle |R_{l,m}|\rangle$ is independent of m. Both of these define ensemble averages. Any particular member of the ensemble will violate these relationships to some degree. These violations matter more for low mode numbers for two reasons: (1) the lowest modes tend to have the biggest amplitudes, and (2) for high mode numbers, there are so many m values that it is more convenient to deal with them statistically. Thus, the relationship between 1-D and 2-D perturbations for a particular capsule is most applicable for the higher modes. Numerical experiments, described below, show that the fitting algorithm in section II is much more accurate in measuring the lower modes than Thus we recommend that the first eight modes be absolutely determined by the fitting procedure described in part II, with the nine great circles. Modes 9 and higher are most conveniently

estimated by averaging together the Fourier spectra of the nine great circles, then using the formalism of Part III to derive a spherical harmonic modal spectrum that is appropriate for a Rayleigh-Taylor model.

V a. Numerical experiments

A typical spectrum of an ICF capsule [5] is shown in Fig. 1. Most of the variance is in the first few modes. We picked the set of 9 great circles defined by the intersection of a sphere with the nine planes x=0, y=0, z=0, x=y, x=z, y=z, x=-y, y=-z and x=-z, with 1024 points in each circle, for a total of 9216 points. Using the spectrum of Fig. 1, we calculated the surface height at each of these 9216 points for the first 100 modes. For each mode n, the 2n+1 spherical harmonics belonging to that mode were given randomly chosen coefficients with a probability proportional to $(1-x^2)^{n-1}$, with -1 < x < 1, and renormalized so that the sum of the squares of the coefficients equaled the spectrum's value at that mode. Thus the total variance was equal to the sum of the spectral values up to mode 100. We added a random gaussian noise with rms σ to each of the 9216 points independently, with σ^2 being the variance due to all modes greater than 100.

Next, we analyzed the resulting surface perturbations in the two ways described above. We fitted the first 8 modes, with 81 independent coefficients, using the matrix inversion described in part II above. We also chose the three great circles defined by the planes x=0, y=0 and z=0 and calculated Fourier spectra for each. The 1-D power spectrum was then taken to be the average of the three power spectra. P_{2D} was then calculated using Eq. (16). We also computed P_{2D} using the nine great circles described above.

Fig. 2 shows the deviation of the computed spectra from the original spectra. The lower curve in red is the result of fitting the first eight modes to the perturbations on the nine great circles. The middle green curve is the computed $P_{\rm 2D}$ from averaging the spectra of nine great circles, and the upper blue curve is the computed $P_{\rm 2D}$ from averaging three great circles, the current way of computing power spectra. The optimal strategy would be to use the nine great circles to compute the first eight modes by the fitting technique (red curve), and compute $P_{\rm 2D}$ from averaging the spectra of the nine great circles.

VI Detection of isolated defects

Suppose there is an isolated defect on a surface of radius r. If we assume for simplicity that this defect is azimuthally symmetric with a shape $f(\theta)$, then we can calculate the spectrum using Eqs. (24), (25) and (26). A great approximation, good for l > 0 and $\theta < \pi/2$, is $P_l(\theta) \approx J_0((l + \frac{1}{2})\theta)$. With this approximation, we have $P_{2D}(l) = \frac{2l+1}{4} \left[\int f(\theta) J_0((l+\frac{1}{2})\theta) \theta d\theta \right]^2$. N of these bumps randomly scattered around the sphere then contribute N times this amount to the variance. For the case of N parabolic bumps of diameter d and height h, we have $P_{2D}(l) = \frac{16Nh^2J_2^2((2l+1)d/4r)}{(2l+1)^3}$, with the largest contributions to modes between l = 0.5 r/d and 3 r/d. Typically, for an ICF capsule with r = 1 mm, the worst case bump has $d = 100 \mu m$, for $l \sim 5-30$ [6]. A great circle will encounter this bump if the center of the bump is within d/2 of the circle. The probability of this happening is about d/2r, or 5% for our example. N great circles will have a probability of encountering the bump of about $Nd/2r - \alpha(Nd/r)^2$, where α is a number of order one that depends on how the great circles intersect. For the nine great circles described above, $\alpha = 0.12$ and the probability of encountering the bump is 40%.

Fig. 3 shows a typical great circle trace on a 2 mm diameter capsule with 50 bumps randomly scattered on the surface, each bump being circular, with a diameter of 100 μ m and a height of 10 μ m. Fig. 4 shows the analytic estimate of the power spectrum, using the equation above, and compares that estimate to two attempts to measure the spectrum with nine great circles. The two red curves are the fits to the first eight modes, and the blue and green spectra are the 2-D spectra that result from transforming the average of the nine power spectra.

Conclusions

The characterization of ICF capsules can be improved by using at least nine great circles to gather surface height data. The first eight modes would be calculated by a least square fit described in section II. Modes nine and larger would be calculated by averaging the nine power spectra obtained from the nine great circles, then using the formulas in section IIIc to compute the two-dimensional power spectrum.

Acknowledgement:

This work was performed under the auspices of the U.S. Department of Energy by the University of California, Lawrence Livermore National Laboratory under Contract No. W-7405-Eng-48.

- [1] Lord Rayleigh, *Scientific Papers* (Cambridge, University Press, Cambridge, England, 1900), Vol. **II**, p. 200
- [2] G.I. Taylor, *Proc. R. Soc. London, Ser. A* **201**, 192 (1950).
- [3] S.W. Haan, *Phys. Rev. A* **39**, 5812 (1989).
- [4] S.M. Pollaine, S. Hatchett, S. Langer, ICF Quarterly Report
- [5] R. Cook, R. McEachern and R. Stephens, Fusion Sci and Technology **35**, 2 (March 1999)
- [6] S.W. Haan et. al., Fusion Sci. and Tech. 41, 164 (2002).